Pion-nucleon scattering from 2 to 5 GeV/c

B. S. Bains
Department of Physics, Punjabi University, Patiala-147002, India
(Received 20 September 1988)

Pion-nucleon scattering is studied for pion laboratory momenta from 2 to 5 GeV/c using a relativistic optical model. $\Pi^{\pm}$-p elastic differential, total elastic, and total cross sections and $\pi^{\pm}$-p polarizations are calculated and compared with the experimental data.

I. INTRODUCTION

At low energies, p_π (pion laboratory momentum) ≤ 2 GeV/c, resonances dominate pion-nucleon scattering; while at higher energies, $p_\pi \geq 5$ GeV/c, diffractive effects dominate. However, in the region between these two momenta structure exists but resonances are not dominant. This region is known as the intermediate energy region. At low energy, $p_\pi \leq 300$ MeV/c, the formation of the $J=T=\frac{3}{2}$ delta resonance[1] explains the scattering. At high energies, Regge pole phenomenology fits the cross sections very well.[2,3] In addition, Regge theory has also been used to fit the differential and total cross-section data in the intermediate energy region at $p_\pi = 3.5$ GeV/c.[2] Since resonances are not dominant in the intermediate energy region, we propose to study π-N scattering in this energy region using a relativistic optical model.[4] This model uses the Bethe-Salpeter equation,[5,6] the relativistic analog of the Schrödinger equation, as a dynamical model. The potential in this model in the ladder approximation arises from the exchange of particles between the nucleon and the pion. In this work, in addition to the exchange of a scalar-isoscalar meson and the ρ meson, we include the exchange of a heavier mass $S^*(980)$ meson. We use for the scalar particle in this model the σ meson of known mass. The Bethe-Salpeter equation is reduced using the techniques of Blackenbecler and Sugar[7] and of Partovi and Lomon.[8] This equation is solved numerically to obtain the scattering amplitudes and hence the cross sections. The parameters in this model are the real and imaginary parts of the coupling constants for the exchanged particles and are adjusted to fit the scattering data.

II. THE BETHE-SALPETER EQUATION FOR THE PION-NUCLEON SYSTEM

The Bethe-Salpeter equation for the pion-nucleon wave function is given by[4]

$$\psi_T(x)=\psi_{0T}(x)-\int d^4y\, G^-(x-y)V_T(y)\psi_T(y)\ , \tag{2.1}$$

where $x=(\mathbf{x},x_0)$ are the relative space-time coordinates. T denotes the isospin of the wave function. For the pion-nucleon system $T=\frac{3}{2}$ or $\frac{1}{2}$. $\psi_{0T}(x)$ is the free Bethe-Salpeter wave function which is given by

$$\psi_{0T}(x)=e^{i\mathbf{k}\cdot\mathbf{x}}U_\lambda(\mathbf{k})\ , \tag{2.2}$$

where $\mathbf{k}$ is the center of mass (c.m.) momentum and $U_\lambda(\mathbf{k})$ is a Dirac spinor.[11] $G^-(x-y)$ is the two-particle Green's function. It is the Fourier transform of $G^-(t)$,

$$G^{\pm}(x-y)=\int \frac{d^4t}{(2\pi)4}e^{it\cdot(x-y)}G^{\pm}(t)\ , \tag{2.3}$$

with $G^{\pm}(t)$ given by

$$G^{\pm}(t)=\frac{m_1-\gamma\cdot t_1}{D^{\pm}(t)}\ , \tag{2.4}$$

where

$$D^{\pm}(t)=(t_1^2+m_1^2\pm i\epsilon)(t_2^2+m_2^2\pm i\epsilon)\ . \tag{2.5}$$

We use a metric

$$t\cdot x=\mathbf{t}\cdot\mathbf{x}-t_0x_0 \tag{2.6}$$

and a representation of the γ matrices given in Ref. 11. The four vectors t_1 and t_2 in Eq. (2.4) are given by

$$t_1=\mu_1 p+t\ ,$$

and

$$t_2=\mu_2 p-t\ , \tag{2.7}$$

where $p=(\mathbf{0},E)$ is the total four momentum in the c.m. system, E is the total c.m. energy, i.e., $E=W_1+W_2$, where $Wi=(\mathbf{k}^2+m_i^2)^{1/2}$ with $i=2$ the pion and $i=1$ the nucleon, μ_1 and μ_2 are

$$\mu_1=\frac{W_1}{E},\quad \mu_2=\frac{W_2}{E}\ . \tag{2.8}$$

$V_T(y)$ in Eq. (2.1) is the Bethe-Salpeter potential in the ladder approximation and is given by

$$V_T(y)=a(T)\left[2\gamma_\mu V^{\mu\nu}(y)\left[i\mu_2 p_\nu-\frac{\partial}{\partial y\nu}\right]\right] +iV(y)+iV_{S^*}(y)\ . \tag{2.9}$$

$V^{\mu\nu}(y)$, $V(y)$, and $V_{S^*}(y)$ are related to the Feynman

propagators for the exchanged particles, i.e., the ρ meson, σ meson, and S^* meson, respectively, and are the Fourier transforms of the functions $V^{\mu\nu}(t)$, $V(t)$, and $V_{S^*}(t)$ given by[4]

$$V^{\mu\nu}(t)=\frac{fg}{t^2+\mu^2-i\epsilon}\left[g^{\mu\nu}-\frac{t^\mu t^\nu}{\mu^2}\right],$$
$$V(t)=\frac{FH}{t^2+\Delta^2-i\epsilon}, \tag{2.10}$$
$$V_{S^*}(t)=\frac{Fs^*Hs^*}{t^2+m_3^2-i\epsilon}.$$

μ, Δ, and m_3 are the masses of ρ, σ, and s^* mesons, respectively, f is the coupling strength of the ρ meson to the nucleon, and g is the coupling strength of the ρ meson to the pion. F and H are the coupling strengths of the σ meson to the nucleon and pion, respectively. Similarly, Fs^* and Hs^* are the coupling strengths of the s^* meson to the nucleon and pion. $g^{\mu\nu}$ is the metric tensor. $a(T)$ in Eq. (2.9) is the eigenvalue of the operator $\mathbf{T}\cdot\mathbf{I}$ where $\mathbf{T}=(T_1,T_2,T_3)$ are the isospin operators of the pion and $\mathbf{I}=(I_1,I_2,I_3)$ are the isospin operators of the nucleon.[12] $a(T)$ has the value

$$a(T)=\begin{cases}\frac{1}{2}, & T=\frac{3}{2},\\ -1, & T=\frac{1}{2}.\end{cases} \tag{2.11}$$

The Fourier transform of (2.1) can be written as

$$\psi_T(t)=\psi_{0T}(t)-iG^-(t)\Gamma_T(t), \tag{2.12}$$

where

$$\psi_{0T}(t)=(2\pi)^4\delta(t_0)\delta^3(\mathbf{t}-\mathbf{k})U_\lambda(\mathbf{k}). \tag{2.13}$$

$\delta(t_0)$ is the Dirac delta function. $\Gamma_T(t)$ is found to be equal to

$$\Gamma_T(t)=\int\frac{d^4q}{(2\pi)4}L_T(t,q)\psi_T(q), \tag{2.14}$$

where

$$L_T(t,q)=2a(T)\Lambda(t,q)+V(t-q)+V_{S^*}(t-q), \tag{2.15}$$

and

$$\Lambda(t,q)=\gamma_\mu(\mu_2 p_\nu-q_\nu)V^{\mu\nu}(t-q). \tag{2.16}$$

Since there is an error in evaluating the Fourier transform of Eq. (2.1) in Ref. 4, our expression for $\Lambda(t,q)$ differs from that found there. From Eqs. (2.12) and (2.14) we obtain the integral equation for $\Gamma_T(t)$

$$\Gamma_T(t)=\Gamma_{0T}-i\int\frac{d^4q}{(2\pi)4}L_T(t,q)G^-(q)\Gamma_T(q) \tag{2.17}$$

with

$$\Gamma_{0T}=\int\frac{d^4q}{(2\pi)4}L_T(t,q)\psi_{0T}(q)$$
$$=L_T(\mathbf{t};\mathbf{k},0)U_\lambda(\mathbf{k}). \tag{2.18}$$

III. RADIAL BETHE-SALPETER EQUATION

After expanding $\psi_T(t)$ and $\Gamma_T(t)$ in terms of spinor spherical harmonics, we obtain an integral equation for the radial function

$$\Gamma_{\xi\delta T}=\Gamma_{0\xi\delta T}(\omega,t_0)+\int\frac{q^2dq}{(2\pi)4}\int dq_0\frac{L_{T\xi}(\omega,t_0;q,q_0)M(q,q_0)}{D^-(q,q_0)}\times\Gamma_{\xi\delta T}(q,q_0), \tag{3.1}$$

where $\omega=|\mathbf{t}|$. The spinor spherical harmonics are given in Rose.[13] $-\xi$ is the eigenvalue of the operator $\sigma\cdot l+1$ where l is the orbital angular momentum operator. δ is the z component of the total angular momentum j,

$$\Gamma_{\xi\delta T}=\begin{bmatrix}\Gamma^+_{\xi\delta T}\\ \Gamma^-_{\xi\delta T}\end{bmatrix}$$

is a two-component quantity, plus and minus signs referring to upper and lower components. $M(q,q_0)$ and $L_{T\xi}(\omega,t_0;q,q_0)$ are 2×2 matrices,

$$M(q,q_0)=\begin{bmatrix}m_1+\omega_1+q_0 & q\\ -q & m_1-\omega_1-q_0\end{bmatrix}. \tag{3.2}$$

$L_{T\xi}$ has elements

$$\begin{aligned}L^{++}_{T\xi}&=2a(T)\Lambda^{++}_\xi-\gamma V_l(\Delta)-\gamma_{S^*}V_l(m_3),\\ L^{+-}_{T\xi}&=2a(T)\Lambda^{+-}_\xi,\\ L^{-+}_{T\xi}&=2a(T)\Lambda^{-+}_\xi,\\ L^{--}_{T\xi}&=2a(T)\Lambda^{--}_\xi-\gamma V_{\bar l}(\Delta)-\gamma_{S^*}V_{\bar l}(m_3),\end{aligned} \tag{3.3}$$

where

$$\begin{aligned}\Lambda^{++}_\xi&=\lambda(\omega_2-q_0)V_l(\mu)+\frac{\lambda(t_0-q_0)}{\mu^2}\{[-q^2+(\omega_2-t_0)(t_0-q_0)]\times V_l(\mu)+\omega qB_l(\mu)\},\\ \Lambda^{+-}_\xi&=-\lambda qV_{\bar l}(\mu)-\frac{\lambda}{\mu^2}\{[-q^2+(\omega_2-t_0)(t_0-q_0)]\times[-\omega V_{\bar l}(\mu)+qV_l(\mu)]-\omega q[\omega B_{\bar l}(\mu)-qB_l(\mu)]\},\\ \Lambda^{-+}_\xi&=\lambda qV_l(\mu)+\frac{\lambda}{\mu^2}\{[-q^2+(\omega_2-t_0)(t_0-q_0)]\times[-\omega V_l(\mu)+qV_{\bar l}(\mu)]-\omega q[\omega B_l(\mu)-qB_{\bar l}(\mu)]\},\\ \Lambda^{--}_\xi&=-\lambda(\omega_2-q_0)V_{\bar l}(\mu)-\frac{\lambda(t_0-q_0)}{\mu^2}\{[-q^2+(\omega_2-t_0)(t_0-q_0)]\times V_l(\mu)+\omega qB_l(\mu)\}.\end{aligned} \tag{3.4}$$

l is the orbital angular momentum; l and $\bar{l}$ are related to ξ through the relations

$$l=\begin{cases}\xi, & \xi>0\ ,\\ -\xi-1, & \xi<0\ ,\end{cases}$$
$$\bar{l}=\begin{cases}-\xi-1=l-1, & \xi>0\ ,\\ -\xi=l+1, & \xi<0\ .\end{cases} \tag{3.5}$$

Positive and negative values of ξ correspond to $j=l\pm\frac{1}{2}$. The coupling parameters γ, λ, and γ_{s^*} are given by

$$\gamma=\frac{FH}{4\pi}\ ,$$
$$\lambda=\frac{fg}{4\pi}\ , \tag{3.6}$$
$$\gamma_{s^*}=\frac{Fs^*Hs^*}{4\pi}\ .$$

$B_l(\mu)$ is given by

$$(2l+1)B_l(\mu)=lV_{l-1}(\mu)+(l+1)V_{l+1}(\mu)\ , \tag{3.7}$$

where

$$V_l(\omega,t_0;q_0,q_0,\mu)=\frac{(4\pi)^2}{2|\mathbf{t}||\mathbf{q}|}Q_l\left[\frac{\mathbf{t}^2+\mathbf{q}^2-(t_0-q_0)^2+\mu^2-i\epsilon}{2|\mathbf{t}||\mathbf{q}|}\right]\ .$$

Q_l is the Legendre function of the second kind.[14] The upper and lower components of $\Gamma_{0\xi\delta T}$ are given in Ref. 4.

IV. THE BLACKENBECLER-SUGAR EQUATION AND SCATTERING AMPLITUDES

Blackenbecler and Sugar[7] and also Partovi and Lomon[8] have developed an approximation to the Bethe-Salpeter equation by replacing the relativistic Green's function with the Green's function which contains the nonrelativistic part. They require that $G(t)$ considered as a function of $\mathbf{k}^2$ should have the same discontinuity across the physical cut[4] as the nonrelativistic Green's function. Using this result and using dispersion relation, Best[4] obtains a new Green's function which leads to the Blackenbecler-Sugar equation

$$\Gamma_{\xi\delta T}(\omega)=\Gamma_{0\xi\delta T}-\int_0^\infty\frac{q^2dq}{2(2\pi)^3E(\mathbf{q})}\frac{L_{T\xi}(\omega,0;q,0)M(q,0)}{q^2-k^2-i\epsilon}\times\Gamma_{\xi\delta T}(q) \tag{4.1}$$

where $\Gamma_{\xi\delta T}(\omega)$ is given by (3.1) with the relative energy variable set equal to zero. Equation (4.1) is a singular integral equation in one dimension which is similar to the Lippman-Schwinger equation[15] found in nonrelativistic scattering theory. This Blackenbecler-Sugar equation leads to scattering amplitudes that obey elastic unitarity if the coupling constants $\gamma,\lambda,\gamma_{s^*}$ are real. However, for complex coupling constants this equation generates a nuclear optical model.

The partial wave scattering amplitudes are related to the solution of Eq. (4.1) through the relation

$$A^T_{l+}(k)=\frac{B}{\sqrt{l+1}}\left[\Gamma^+_{\xi(1/2)T}(k,0)+\frac{k}{\omega_1+m_1}\Gamma^-_{\xi(1/2)T}(k,0)\right],\quad \xi<0\ , \tag{4.2}$$
$$A^T_{l-}(k)=-\frac{B}{\sqrt{l}}\left[\Gamma^+_{\xi(1/2)T}(k,0)+\frac{k}{\omega_1+m_1}\Gamma^-_{\xi(1/2)T}(k,0)\right],\quad \xi>0\ ,$$

where

$$B_1=\frac{m_1}{4\pi E}\left[\frac{\omega_1+m_1}{8\pi m_1}\right]^{1/2}\ .$$

δ and λ have been set equal to $\frac{1}{2}$. $l_\pm$ correspond to $j=l\pm\frac{1}{2}$. The cross section and polarization formulas for π-p interactions are given in Refs. 16 and 17.

V. NUMERICAL ANALYSIS AND RESULTS

In this section, we give the numerical results of our calculations for cross sections and polarizations. Equation (4.1) is hard to solve analytically; instead we solve it numerically. We use Simpson's rule[18] with a total of 31 mesh points, 11 from 0 to $2k$, including the origin and 20 from $2k$ to $\bar{k}$. As in Ref. 4, in order to examine the cutoff dependence of the upper limit in the integral in Eq. (4.1), we evaluated the partial wave scattering amplitudes for $\bar{k}$ varying from 10.15 to 22.56 GeV/c and found that the amplitudes changed only by 2 parts in 10^4 as $\bar{k}$ is increased from 10.15 to 22.56 GeV/c. Hence we choose 22.56 GeV/c as the cutoff value for $\bar{k}$. Table I shows the cutoff dependence of our $\xi=-1$ and $\xi=-3$ phase shifts. For each isospin channel we calculated 17 partial wave amplitudes in order to determine the cross sections and polarizations.

The real part of the coupling parameters for the σ particle and s^* meson were calculated using the relation[19]

$$g_{\sigma NN}g_{\sigma\pi\pi}=\frac{g^2_{N\pi\pi}}{2m_N}(m_\sigma^2-m_\pi^2)\ , \tag{5.1}$$

where $g_{N\pi\pi}$ is the pion-nucleon coupling constant. Here m_σ, m_π, and m_N are the masses of the σ particle, the pion, and the nucleon, respectively. The mass of the σ particle is taken to be 550 MeV (Ref. 19) and the s^* is 980 MeV.[20] We take the ρ parameters same as in Ref. 4. For real coupling parameters, the partial wave scattering

TABLE I. Phase shifts (degrees) at $k=0.938$ GeV/c vs cutoff momentum $\bar{k}$. $\gamma=\gamma_{s^*}=0$, Re$\lambda=2.0$, Im$\lambda=0$.

$\bar{k}$ (GeV/c)	$\xi=-1$	$\xi=-3$
10.15	43.395	4.946
14.29	43.658	4.922
22.56	43.557	4.854

TABLE II. The coupling parameters γ, λ, and γ_{s^*}. γ and γ_{s^*} are in GeV.

p_π (GeV/c)	Reγ (GeV)	Imγ (GeV)	Reλ	Imλ	Reγ_{s^*} (GeV)	Imγ_{s^*} (GeV)
2	−2.16	5.0	1.0	0.4	−7.17	1.0
3	−2.16	8.0	1.0	0.4	−7.17	1.0
5	−2.16	15.0	1.0	0.4	−7.17	1.0

amplitudes satisfy the elastic unitarity condition.[21] This condition is

$$\sum_{\lambda'} \int d\Omega_{k'} |f^T_{\lambda'\lambda}|^2 = \frac{4\pi}{k} \mathrm{Im} f^T_{\lambda\lambda}(\mathbf{k},\mathbf{k}) , \tag{5.2}$$

or

$$|A^T_{l\pm}|^2 = \frac{\mathrm{Im}\, A^T_{l\pm}(k)}{k} .$$

We tested these relations and found that the imaginary parts of the phase shifts were different from zero by about 5 parts in 10^{15}. We also compared our phase shifts and inelasticities at $p_\pi = 3.14$ GeV/c with that of Zia.[22] We found quite good agreement with his calculations, although his solutions are based on a variational principle[21] and Wick rotation[23] methods. These calculations demonstrate the accuracy of our results.

In order to fit scattering data using this relativistic optical model we first adjusted the imaginary parts of the σ particle and s^* meson coupling parameters at $p_\pi = 5$ GeV/c to fit the experimental cross-section data. The results are shown in Figs. 5 and 6. In the rest of the calculations, we varied only the imaginary part of γ as the laboratory momentum changed from 2 to 5 GeV/c. This increase in the imaginary part of γ models pion absorption into other inelastic channels. Since there is a negative sign in the second term of Eq. (2.1), we keep the imaginary part of the coupling parameters positive in order to correspond to absorption. For complex coupling parameters, the imaginary part of our scattering amplitudes was positive. Table II gives our values of the coupling parameters, i.e., γ, λ, and γ_{s^*}. With our coupling parameters,

TABLE III. π^+-p total elastic and total cross sections at $p = 2$, 2.92, and 5 GeV/c. The experimental data are from Ref. 26.

p_π (GeV/c)	Total elastic cross section (mb)	Experimental values (mb)	Total cross section (mb)	Experimental values (mb)
2	9.544	9.100 ±2.000	28.811	29.070 ±0.040
2.92	8.023	5.100 ±1.000	28.277	28.700 ±0.500
5	7.349	5.85 ±0.180	26.617	26.49 ±0.140

TABLE IV. π^--p total elastic and total cross sections at $p_\pi = 2$, 3, and 5 GeV/c. The experimental data are from Ref. 26.

p_π (GeV/c)	Total elastic cross section (mb)	Experimental value	Total cross section (mb)	Experimental value
2	8.301	8.000 ±1.500	30.038	35.800 ±0.400
3	7.613	6.700 ±1.300	29.530	31.940 ±0.160
5	7.970	6.500 ±1.300	28.826	28.580 ±0.200

we find quite good agreement with the experimental total elastic and total $\pi^\pm$-p cross sections. The results are shown in Tables III and IV. Except for the dip near $t = 0.6$ (GeV/c)^2, for p_π between 2 and 4 GeV/c, this model gives quite good agreement with the forward diffraction peak in the elastic differential cross-section data. We present our calculations in the accompanying figures (Figs. 1–10) for three different pion laboratory momenta, i.e., $p_\pi = 2.07$, 3, and 5 GeV/c in this inter-

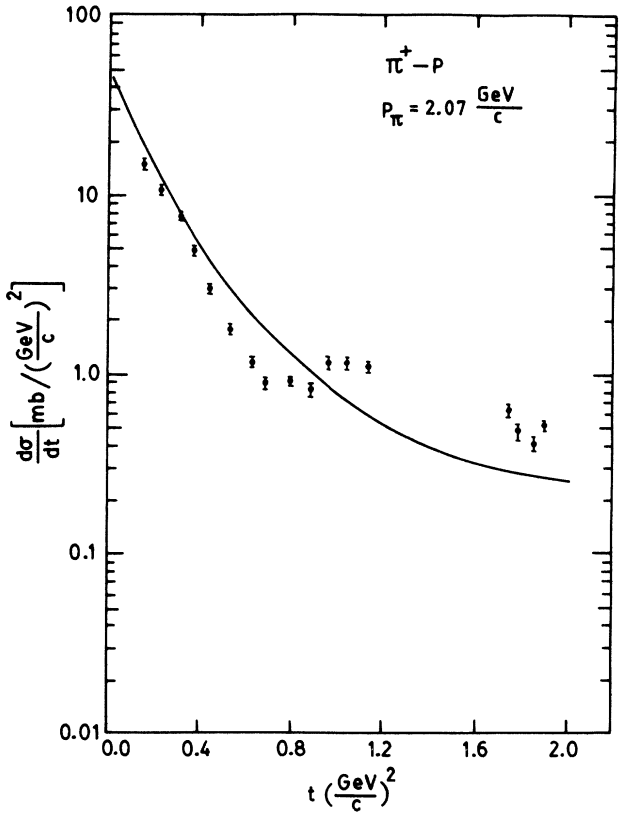

FIG. 1. Fit to the π^+-p differential cross-section data at $p_\pi = 2.07$ GeV/c. The parameters are from Table II. The experimental data are from Ref. 9. t is the four momentum transfer squared, i.e., $t = 2k^2(1-\cos\theta)$ and θ is the c.m. scattering angle.

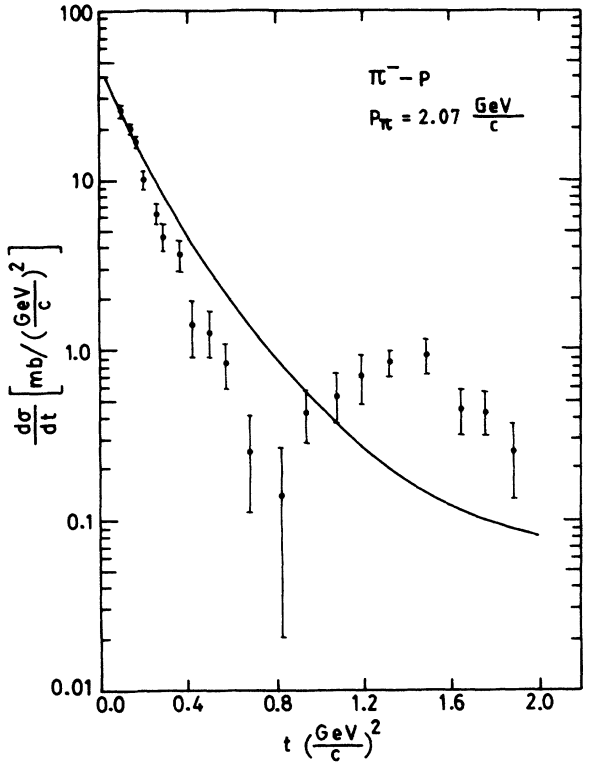

FIG. 2. Fit to π^--p differential cross-section data at $p_\pi = 2.07$ GeV/c. The experimental data are from Ref. 9.

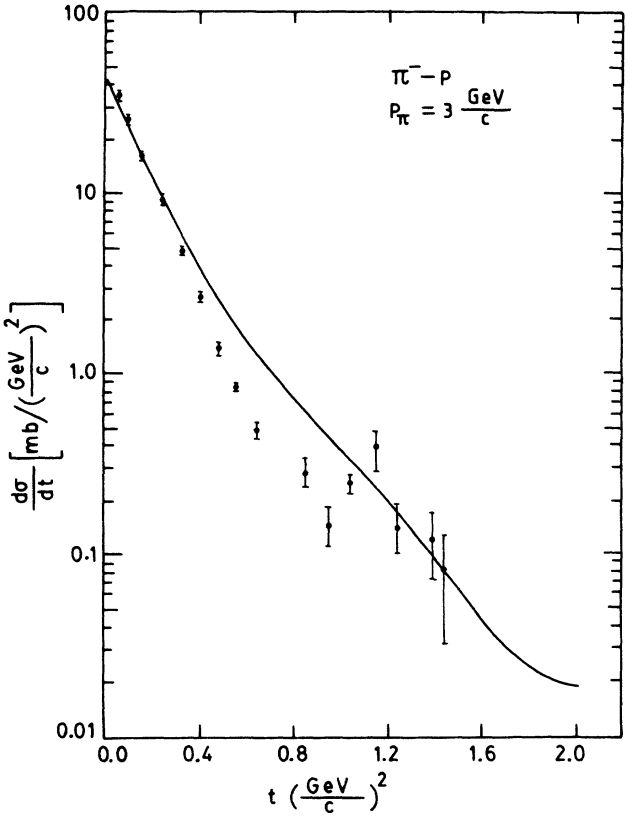

FIG. 4. Fit to π^--p differential cross-section data at $p_\pi = 3$ GeV/c. The experimental data are from Ref. 10.

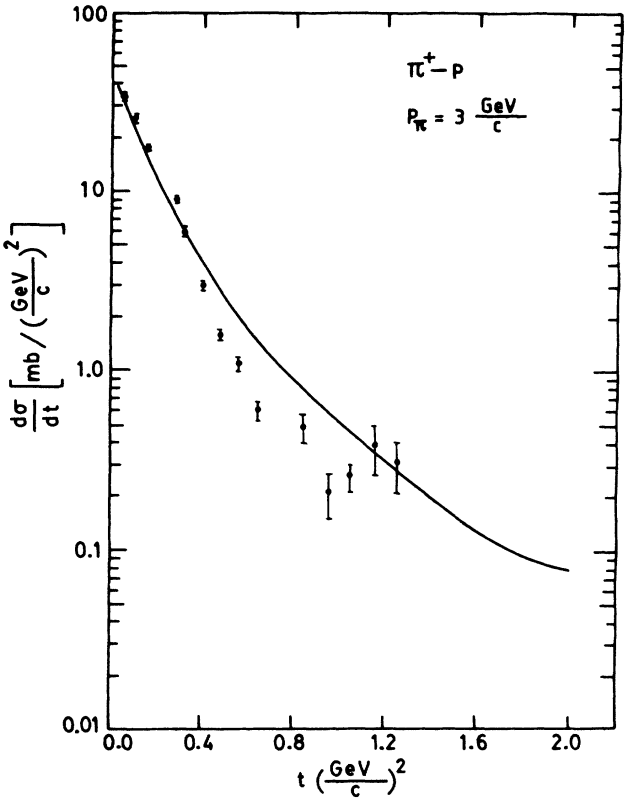

FIG. 3. Fit to π^+-p differential cross-section data at $p_\pi = 3$ GeV/c. The experimental data are from Ref. 10.

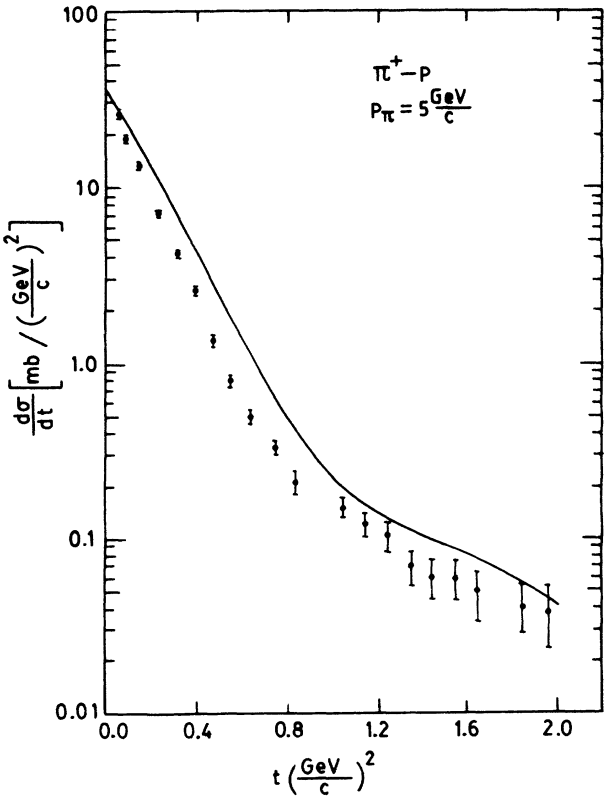

FIG. 5. Fit to π^+-p differential cross-section data at $p_\pi = 5$ GeV/c. The experimental data are from Ref. 10.

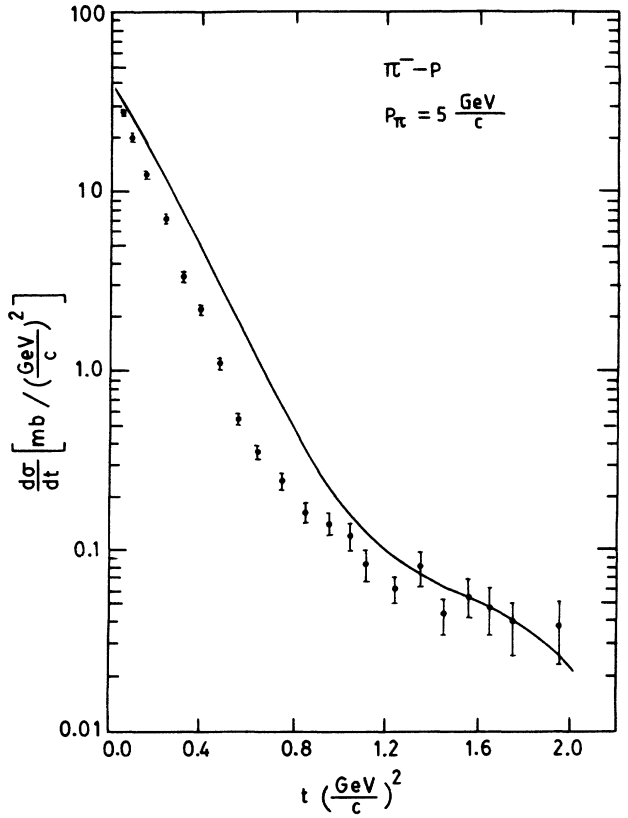

FIG. 6. Fit to π^--p differential cross-section data at $p_\pi = 5$ GeV/c. The experimental data are from Ref. 10.

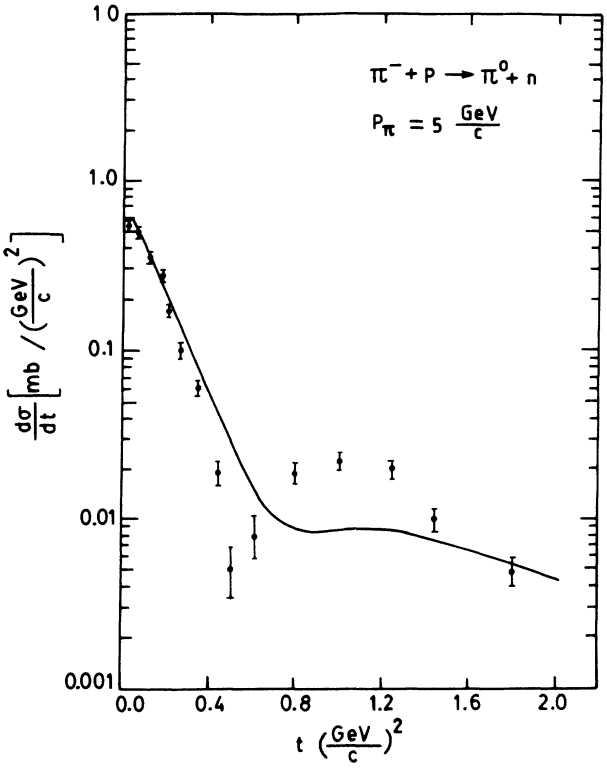

FIG. 8. Fit to the charge exchange differential cross-section data at $p_\pi = 5$ GeV/c. The experimental data are from Ref. 25.

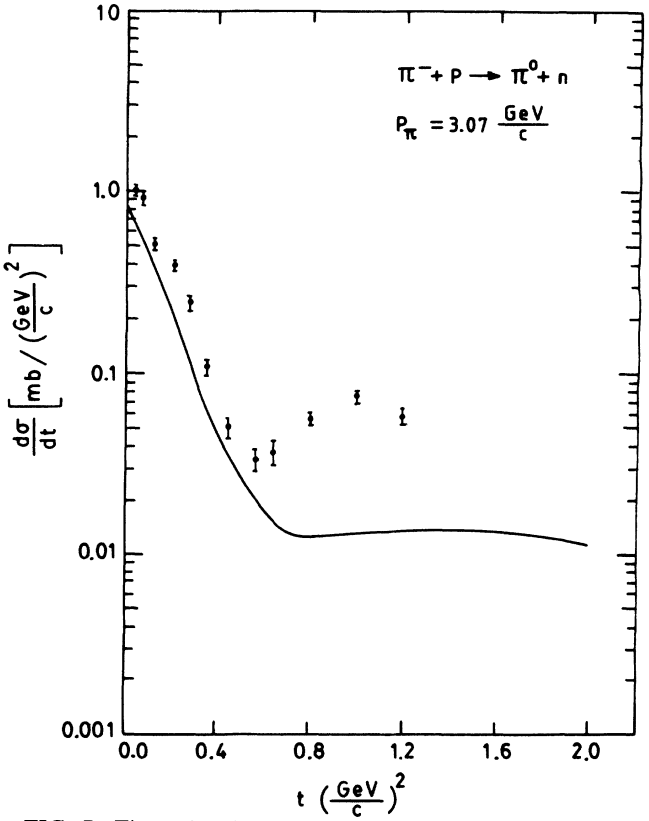

FIG. 7. Fit to the charge exchange differential cross-section data at $p_\pi = 3.07$ GeV/c. The experimental data are from Ref. 25.

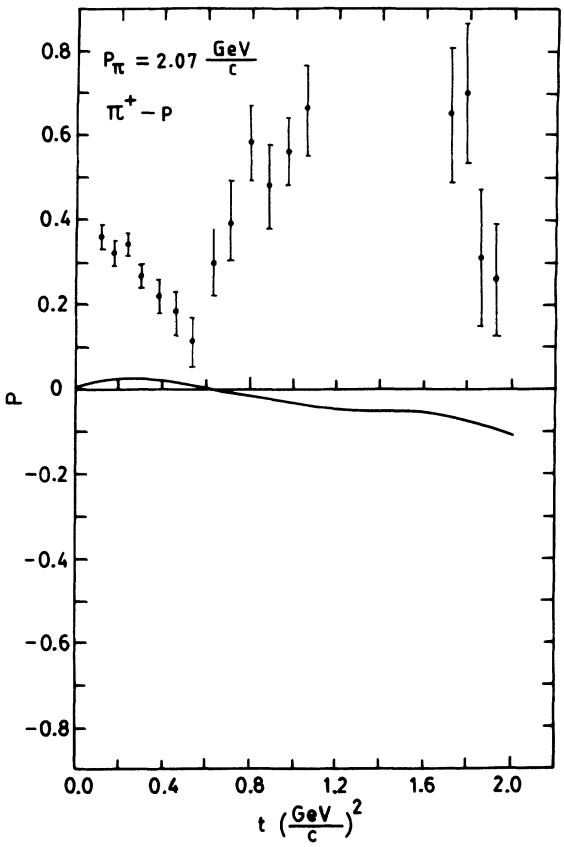

FIG. 9. Fit to the π^+-p polarization at $p_\pi = 2.07$ GeV/c. The experimental data are from Ref. 25.

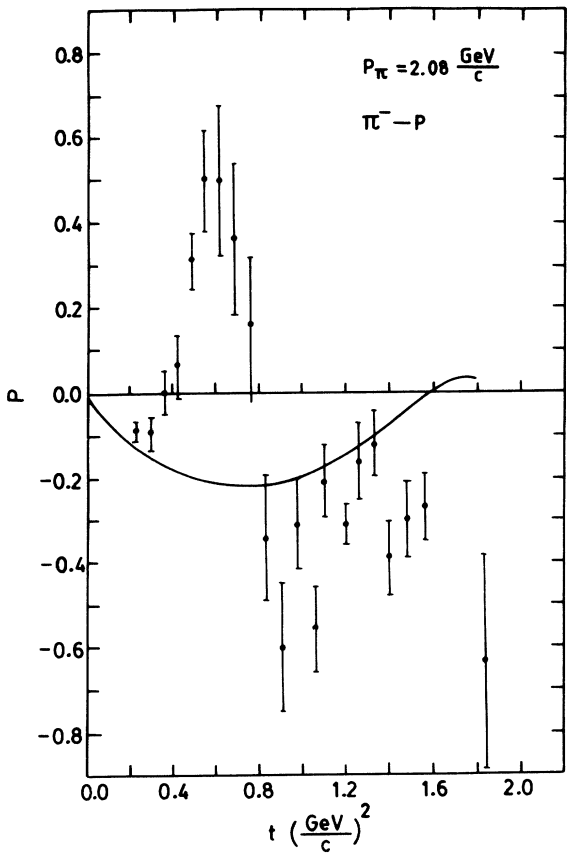

FIG. 10. Fit to the π^--p polarization at $p_\pi = 2.08$ GeV/c. The experimental data are from Ref. 25.

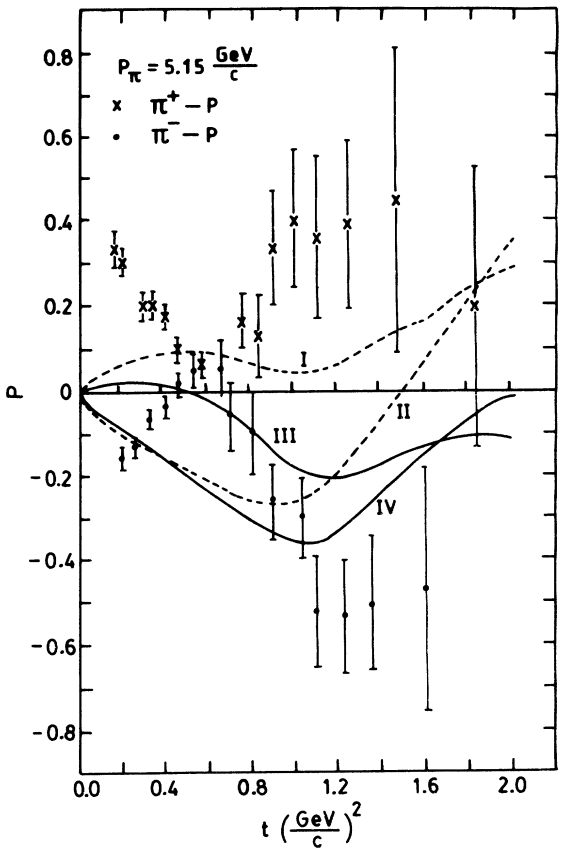

FIG. 11. Fit to the $\pi^{\pm}$-p polarization at $p_\pi = 5.15$ GeV/c. The dashed curves correspond to $\mathrm{Re}\lambda = 1.5$ and $\mathrm{Im}\lambda = 0.6$. The experimental data are from Ref. 24. The different curves are as follows: Curve I $= \pi^+$-p, Curve II $= \pi^-$-p, Curve III $= \pi^+$-p, and Curve IV $= \pi^-$-p.

mediate energy region. Our calculations show only qualitative agreement with the experimental $\pi^{\pm}$-p polarization. The sign of the $\pi^{\pm}$-p polarization agrees only up to $t \sim 0.5$ (GeV/c)^2. However, we find that by slightly changing the ρ parameters, we can get better agreement for $\pi^{\pm}$-p polarizations. As an example, see Fig. 11 for our calculations at $p_\pi = 5.15$ GeV/c for the two different values of the ρ parameters. We also find that the charge exchange data is also fitted well (Figs. 7 and 8) by this model.

VI. CONCLUSION

In conclusion, we find that the relativistic optical model gives a good fit to the forward diffraction peak in the differential elastic cross-section data. Except for the dip near $t \sim 0.6$ (GeV/c)^2, we find a reasonably good fit for momentum transfers up to $t = 2$ (GeV/c)^2. Also our calculations for $\pi^{\pm}$-p total elastic and total cross sections agree well with the experimental values. The polarizations agree only qualitatively. Improved fits to large angle scattering might be achieved if the exchange of a heavier mass particle, for example, the $f_0(1260)$ mass, were included into the potential.

[1]G. F. Chew and F. E. Low, Phys. Rev. **107**, 1570 (1956).
[2]V. Barger and R. J. N. Phillips, Phys. Rev. Lett. **22**, 116 (1969).
[3]S. Frautschi and B. Margolis, Nuovo Cimento **A56**, 1155 (1968).
[4]Melvyn E. Best, Ann. Phys. (N.Y.) **69**, 400 (1972).
[5]H. Bethe and E. Salpeter, Phys. Rev. **84**, 1232 (1951).
[6]M. Gellmann and F. E. Low, Phys. Rev. **84**, 350 (1951).
[7]R. Blackenbecler and R. Sugar, Phys. Rev. **142**, 1051 (1966).
[8]H. M. Partovi and E. L. Lomon, Phys. Rev. D **2**, 1999 (1970).
[9]C. T. Coffin *et al.*, Phys. Rev. **159**, 1169 (1967).
[10]I. Imbats *et al.*, Phys. Rev. D **9**, 1179 (1974).
[11]I. J. R. Aitchison, *Relativistic Quantum Mechanics* (Barnes & Noble, New York, 1972).
[12]Stephen Gasiorowicz, *Elementary Particle Physics* (Wiley, New York, 1966).
[13]M. E. Rose, *Relativistic Electron Theory* (Wiley, New York,

1961).
[14]P. M. Morse and H. Feshback, *Methods of Theoretical Physics* (McGraw-Hill, New York, 1953).
[15]S. Schweber, *An Introduction To Relativistic Quantum Field Theory* (Harper and Row, New York, 1961).
[16]Bransden and Moorhouse, *The Pion-Nucleon System* (Princeton University, Princeton, 1973).
[17]J. J. Sakurai, *Invariance Principles and Elementary Particles* (Princeton University, Princeton, 1964), Appendix A.
[18]M. M. Abramowitz and I. A. Stegun, *Handbook of Mathematical Functions* (U.S. Government Printing Office, Washington, D.C., 1964).
[19]M. D. Scadron, *Advanced Quantum Theory and Its Applications Through Feynman Diagrams* (Springer-Verlag, New York, 1979).
[20]Particle Data Group, Lawrence Berkeley Laboratory, 1982.
[21]S. Schwartz and C. Zemach, Phys. Rev. B **141**, 1454 (1966).
[22]R. Zia, Ph.D. thesis, MIT, 1968 (unpublished).
[23]G. Wick, Phys. Rev. **96**, 1124 (1954).
[24]R. J. Esterling *et al.*, Phys. Rev. Lett. **21**, 1410 (1963).
[25]L. B. Series, in *Scattering of Elementary Particles*, edited by H. Schopper (Springer-Verlag, New York, 1973).
[26]E. Bracci *et al.*, *Compilation of cross sections, π^- and π^+ Induced Reactions* (CERN, Geneva, 1972).